

# SIMULATION OF CONTACT PROBLEMS IN RAILWAY ENGINEERING

Roman Bogacz<sup>1</sup> and Czesław Bajer

*Institute of Fundamental Technological Research,  
Polish Academy of Sciences,  
Świętokrzyska 21, 00-049 Warsaw, Poland*

## Abstract

In the paper results of the analysis of high frequency forced vibration of rolling wheelset interacting with rail by means of springs carrying the the loading in three directions of relative displacements (vertical, lateral and longitudinal) and a spin which models rotational resistance are presented. A wheelset is modelled as a system of two elastic wheels connected by a rigid axle. Wheel tires are modelled as a elastic Rayleigh's beams with constant curvature, joined with the axle by continuous, visco-elastic Winkler-type foundation.

The second approach was performed by the space-time discrete modeling of the dynamic rail-wheel contact problem. The space-time finite element method was applied to the analysis of the induced corrugations. An arbitrary mesh modification, both in time and space, enables the easy modeling of rapidly varying contact zone. The velocity formulation is used and the discontinuity of the velocity in the contact is removed by a special algorithm. Finally the discussed technique was used to simulate interaction of the elastic wheel and rigid rail. It was shown that the contact force oscillates and the material of the wheel rotates oscillatory.

## 1 Introduction

In the railway transportation both the load carrying capacity of carriages and speed of trains increase. It causes new problems of exploitation: faster wear of rail surfaces and wheel tires. Circular geometry of wheels and plane surface of rail heads lose their perfection. Both on the rail head and the wheel ring wave-shape deformations can be observed. They are called corrugations. Even in low speed motion and light trains the result of successful deformation of steel rail by the wheel can be seen by the naked eye and requires frequent intervention of technical services. The improper wear results in considerable increase of noise. In cities noise

generated by tramways or even underground trains negatively effects the environment. In long distance trains can be tiring for passengers. From the technological point of view spurious effects of mechanical phenomena shorten the life of large steel parts of mentioned mean of transportation.

Another case where similar phenomenon occurs are vehicle breaks and clutches. High frequency oscillations generated between break shoes and disks or friction disks of the clutch considerably reduce the life time of elements. Besides a noise affects the environment by tones heavy to carry down.

The aim of the work is the simulation and investigation of generation of corrugations and its influence on the durability of rails. Particularly burdensome conditions will be in the scope: self excitation in higher (300 km/h) velocity range, influence of non-linear material properties (visco-plasticity), non-linear friction, torsional vibration of wheel/axle system, influence of plate bending state for cone-shaped wheel, approach to optimization of resulting parameters. The subject is wide and several research centers in the world work intensively in the field.

Both the polygonized contour of the wheel and the waved surface of the rail will be simulated in the selected tasks. The process of the destruction of wheels and rails will be investigated.

The problem pointed is wide and has been undertaken in several research and technological centers in the world (USA, Japan, Germany, France). Different hypotheses were assumed as a base of investigation. Some of them can be easily rejected, others require intensive theoretical and numerical tests. In the literature the following cases are pointed as a source of corrugations:

- imperfections in rail joints,
- cone form of wheels which results in different linear

---

<sup>1</sup>and Warsaw University of Technology

speed of left and right wheel; it causes snaking of trains and generally, disturbs steady motion,

- periodical structure of rails (sleepers); instability of motion on the periodically placed supports [1],
- contact problems between wheel and rail; stick and slip sections which vary with high frequency (horizontally) generate waves which deform elastically, then plastically metal surfaces [2, 3, 4],
- residual stress caused by manufacturing and service of rails and wheels [5],
- non-linear friction law in the stick zone [3],
- influence of material hardening [6],
- deformation of elements of wheel/axle as results of impact during rolling motion,
- instability of wheelsets motion [7, 8].

## 2 Simple truck models

Theoretical formulations which are intended to provide calculation models are generally limited to influencing factors which seem to be important. The particular significance of dynamic problems explains why increasing attention has been paid to the study of oscillations with the aid of theoretical calculation models which give a better insight into the phenomenon of corrugation formation.

The most significant fact is rail or wheel tire vibration under the action of moving and oscillating load. Bogacz *et al.* [9] examined the rail modelled as the Bernoulli-Euler or Timoshenko beam on an elastic foundation subjected to a moving oscillating force.

The equations of the Timoshenko beam motion regarding the effects of shear deformation and rotary inertia are given as follows:

$$\begin{aligned}
 EI \frac{\partial^2 \psi}{\partial x^2} + \kappa AG \left( \frac{\partial w}{\partial x} - \varphi \right) - \rho I \frac{\partial^2 \psi}{\partial t^2} &= 0 \\
 \kappa AG \left( \frac{\partial^2 w}{\partial x^2} - \frac{\partial \varphi}{\partial x} \right) - \rho A \frac{\partial^2 \psi}{\partial t^2} - b \frac{\partial w}{\partial t} - cw &= F_0 \delta(x - vt) e^{i\omega t}
 \end{aligned} \quad (1)$$

The solution of (1) can be written in the form:

$$W(R_0, \tau) = W_1(R_0) \cos \omega \tau + W_2(R_0) \sin \omega \tau \quad (2)$$

The solution and discussion of essential differences between the solutions for various velocities  $V$  and frequencies  $\Omega$  are given by Bogacz *et al.* [9]. An example of

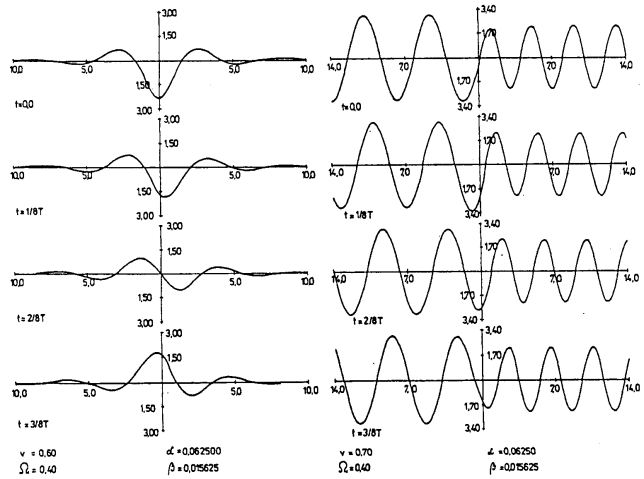


Figure 1: Displacement of the beam.

displacements for  $t = 0$ ,  $t = T/8$ ,  $t = T/4$ ,  $t = 3T/8$ ,  $t = 2\pi/\omega$  is presented in Fig. 1.

## 3 Dynamic stability of the wheel

### 3.1 Physical and mathematical model of the wheel

The wheel tire is modeled by the elastic curved Rayleigh's beam joined with the axle by means of the continuous elastic Winkler type foundation. The elastic foundation constituting the wheel disc carries out the load in three directions: circumferential, radial and vertical to the plane of the wheel. Curved beam theory ensures the real shape of the cross-section. Visco-elastic properties of the wheel material are described by the Kelvin-Voigt model

$$q_j = - \left( k_j u_{0j} + c_j \frac{\partial u_{0j}}{\partial t} \right) \quad (3)$$

where  $q_j$ ,  $u_{0j}$ , ( $j = 1, 2, 3$ ) – reactions and displacements of elastic foundation in circumferential, radial and vertical direction,  $k_j$ ,  $c_j$  – stiffness and damping in elastic foundation. The following coordinate systems are assumed in the 3-D mathematical model of rotating railway wheel (2):

- polar system  $\varphi, R$  with the pole in the wheel center, rigidly connected with the rotating wheel; by means of three coordinates the geometrical axis of the tire has been described,
- polar system  $\varphi_1, R$ , with a pole in the wheel center,

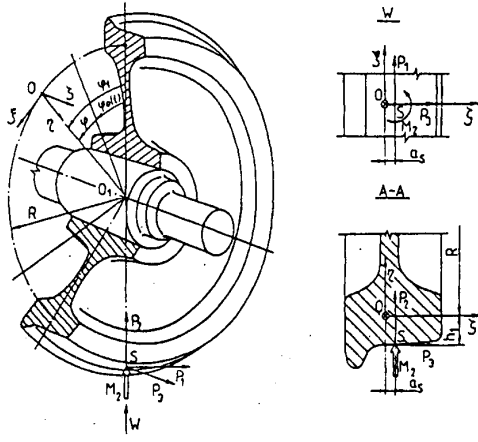


Figure 2: Coordinate systems and exciting forces.

used for the description of the rotational motion of the wheel,

- rectangular system of coordinates  $\xi, \eta, \zeta$  with the origin  $O$  on geometrical axis of the tire and a position given by spatial coordinates  $\varphi$  or  $\varphi_1$ ;  $\xi, \eta, \zeta$  constitute tangential, normal and binormal directions to the undeformed axis of the wheel; this coordinate system allows to describe displacements, internal and external forces and a cross-section of the wheel tire.

The geometrical axis of the wheel tire were modified by the geometrical centers of gravity of undeformed wheel-tire cross-sections. Assuming the angular velocity of the wheel  $\dot{\varphi}$  to be constant, the relation between  $\varphi, R$  and  $\varphi_1, R$  has the following form:

$$\varphi_1 = \varphi + \dot{\varphi}_0 t \quad (4)$$

The problem is more complex now due to the the curved beam and greater number of dimensions. Detailed examination of the of the problem in the case of two dimensions was described in [10].

The system of coupled differential equations which describe forced vibrations of the wheel tire rotating with the velocity  $\dot{\varphi}_0$ , including visco-elasticity can be written in polar coordinates  $\varphi, R$  in the form:

$$\begin{aligned} & \frac{\partial^2}{\partial t^2} \left[ \frac{\partial}{\partial \varphi} (-m_1 v + m_2 w) + m_3 u \right] + \frac{\partial}{\partial t} \left[ \frac{\partial}{\partial \varphi} (-a_1 \frac{\partial u}{\partial \varphi} \right. \\ & \left. + a_2 v + a_3 w) + a_4 u - 2\dot{\varphi}_0 (m_4 v + s_1 \vartheta) \right] \\ & + \frac{\partial}{\partial \varphi} \left( -k_1 \frac{\partial u}{\partial \varphi} + k_2 v - k_3 w \right) = R q_\xi + m_\xi \quad (5) \\ & \frac{\partial^2}{\partial t^2} \left[ \frac{\partial}{\partial \varphi} (-m_5 v + m_6 w) - m_7 \frac{\partial u}{\partial \varphi} - m_8 v - s_2 \vartheta \right] + \end{aligned}$$

$$\begin{aligned} & \frac{\partial}{\partial t} \left\{ -a_5 \frac{\partial^4 v}{\partial \varphi^4} + \frac{\partial^2}{\partial \varphi^2} [(-2a_5 + a_6)v + a_7 w] + a_2 \frac{\partial u}{\partial \varphi} \right. \\ & \left. - (a_5 + a_8)v + d_1 \vartheta + 2\dot{\varphi}_0 \left[ \frac{\partial}{\partial \varphi} (m_9 v - m_{10} w - s_3 \vartheta) \right. \right. \\ & \left. \left. - m_{11} u \right] \right\} - k_5 \left( \frac{\partial^4 v}{\partial \varphi^4} + 2 \frac{\partial^2 v}{\partial \varphi^2} + v \right) - \frac{\partial^2}{\partial \varphi^2} \left( k_6 \frac{\partial^2 w}{\partial \varphi^2} \right. \\ & \left. - k_7 v - k_8 w - t_1 \vartheta \right) + k_2 \frac{\partial u}{\partial \varphi} - k_9 v + t_2 \vartheta \\ & = -R q_\eta + \frac{\partial m_\xi}{\partial \varphi} + s_8 \dot{\varphi}_0^2 \quad (6) \end{aligned}$$

$$\begin{aligned} & \frac{\partial^2}{\partial t^2} \left[ \frac{\partial^2}{\partial \varphi^2} (m_{12} v + m_{13} w) + m_{14} \frac{\partial u}{\partial \varphi} - m_{15} w - s_4 \vartheta \right] + \\ & \frac{\partial}{\partial t} \left[ -a_9 \frac{\partial^4 v}{\partial \varphi^4} + \frac{\partial^2}{\partial \varphi^2} (a_7 v + a_{10} w + d_2 \vartheta) - a_3 \frac{\partial u}{\partial \varphi} \right. \\ & \left. - a_{11} w - d_3 \vartheta - 2\dot{\varphi}_0 \frac{\partial}{\partial \varphi} (m_{16} v - s_5 \vartheta) - \frac{\partial^4 v}{\partial \varphi^4} (k_6 v \right. \\ & \left. + k_{10} w) + \frac{\partial^2}{\partial \varphi^2} (k_8 v + k_{11} w + t_3 \vartheta) - k_3 \frac{\partial u}{\partial \varphi} - k_{12} w \right. \\ & \left. - t_4 \vartheta = -R q_\xi + \frac{\partial m_\eta}{\partial \varphi} \right. \\ & \left. \frac{\partial^2}{\partial t^2} (m_{17} v + m_{18} w + s_6 \vartheta) \right. \\ & \left. + \frac{\partial}{\partial t} \left\{ -\frac{\partial^2}{\partial \varphi^2} (a_{12} w + d_4 \vartheta) - a_{13} v + a_{14} w + d_5 \vartheta + \right. \right. \\ & \left. \left. 2\dot{\varphi}_0 \left[ \frac{\partial}{\partial \varphi} (m_{12} v + m_{13} w) + m_{14} u \right] \right\} - \frac{\partial^2}{\partial \varphi^2} (k_6 v \right. \\ & \left. + k_{13} w + t_5 \vartheta) - k_{14} v + k_{15} w + t_6 \vartheta = m_\xi - s_9 \dot{\varphi}_0^2 \quad (7) \end{aligned}$$

where:

- $u, v, w$ —displacements of point  $O$  in directions  $\xi, \eta, \zeta$ ,
- $\vartheta$ —rotation angle of the wheel tire cross-section related to  $\xi$  direction,
- $m_i$ —reduced masses of the wheel tire of the disc,
- $s_i$ —reduced mass moments of the first order,
- $k_i, t_i$ —wheel tire and disc reduced stiffness,
- $a_i, d_i$ —damping equivalent coefficients of the wheel tire and disc,
- $q_\xi, q_\eta, q_\zeta$ —external forces distributed continuously along the geometrical axis of the wheel tire,
- $m_\xi, m_\eta, m_\zeta$ —external moments distributed continuously along the geometrical axis of the wheel tire.

The system of equations (7) is the mathematical 3-dimensional model of the wheel rotating with the velocity  $\dot{\varphi}_0$ . The first two equations refer to the motion of the wheel tire in its plane (circumferential and flexural

radial vibrations). The vibrations in the wheel plane and vibrations out of the wheel plane are coupled by means of elastic and inertial forces.

Vibrations are excited by harmonic point forces acting at the contact point  $S$ . Spin moment  $M_2$  was also taken into account as a source of excitation. The positive senses of exciting force was assumed according to the senses of axes  $\xi, \eta, \zeta$  (Fig. 2). The solution of the system of equations (7) describing forced vibration of the rotating wheel is postulated in the coordinate system  $\varphi, R$  in the form:

$$u(\varphi, t) = \frac{1}{2\pi}T_{10}(t) + \frac{1}{\pi} \sum_{n=1}^{\infty} T_{11}(t)\cos n\varphi_1 + T_{12}(t)\sin n\varphi_1 \quad (8)$$

The amplitude  $A_w$  of vibration of point  $O$  can be expressed as follows:

$$A_w(\varphi_1) = \frac{1}{\pi} \left\{ \left[ \frac{a_0}{2} + \sum_{n=1}^{\infty} (a_{1n}\cos n\varphi_1 + a_{2n}\sin n\varphi_1) \right]^2 + \left[ \frac{b_0}{2} + \sum_{n=1}^{\infty} (b_{1n}\cos n\varphi_1 + b_{2n}\sin n\varphi_1) \right]^2 \right\} \quad (9)$$

The displacements  $v, w, \vartheta$  and the amplitudes  $A_v, A_w, A_\vartheta$  are found in the same way.

### 3.2 Numerical results

Frequency response functions obtained by numerical calculations in the case of forced vibrations of the railway wheel is depicted in Fig. 3. Characteristics refer to the the point  $O$  for the coordinate  $\varphi_1 = \pi$ . Amplitudes  $A_w(\pi), A_v(\pi), A_\vartheta(\pi)$  were determined for the first eleven modes of vibrations and their values were given in dB assuming the reference level  $10^{-11}$  m.

The numerical analysis was performed for the nominal wheel diameter 0.95 m and for the angular velocities  $\dot{\varphi}_0$  of the wheel which correspond to the linear velocities 0, 200 and 400 km/h in the rolling motion. Other numerical results can be found in [11].

In the case of the velocity about 200 km/h the amplitude with the frequency about 100 Hz are considerably higher then in the case 0 km/h of 400 km/h.

## 4 Space-time element analysis

### 4.1 The space-time modeling of contact problem

Dynamic contact problems are characteristic of fast varying contact domains. In some problems the pre-

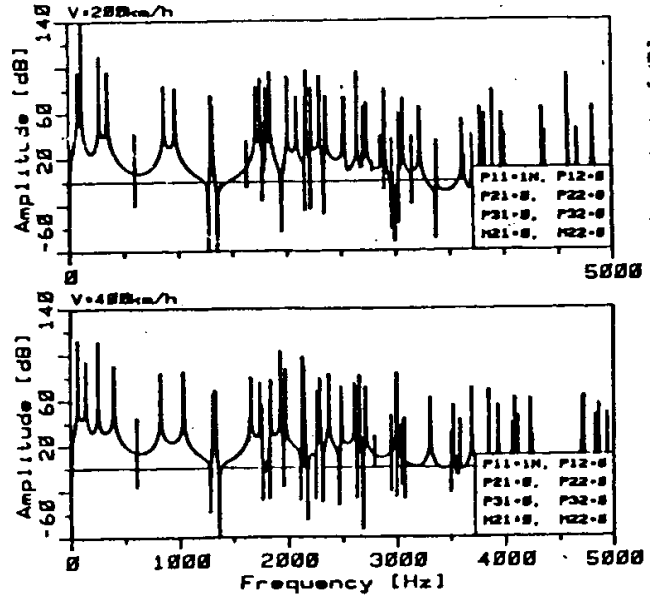


Figure 3: Frequency response functions for rotating railway wheel.

cise definition of the contact zone is of fundamental importance. Contact phenomena with friction that involve vibration of the stick and slip type require both the small time step of the integration of the differential equation of motion and refined mesh in that region. The finite element method gained its popularity since it is relatively simple and universal in applications. However, in certain problems the F.E.M. is difficult since its discrete form does not allow to investigate the problem with the required precision. For example, the varying contact zone, extended between two nodes in spatial mesh requires subintegration of resulting matrices to evaluate more precisely friction contribution. Much more natural approach is to modify the spatial mesh and subintegrate the differential equation in time, in required regions only.

The spatial adaptation of the mesh in structural dynamics can rarely be found in the literature (for example [12, 13, 14]). However, the simplest interpolation of displacement, velocity and acceleration vectors were discussed there with particular reference to additional joint. Such a discontinuous path to the refined/coarsened mesh changes the problem under consideration: local and global stiffness and temporary distribution of acceleration and velocity, compared with the problem solved with the constant mesh. The adaptation procedure may incorporate greater error than the simple classical computation. It is well visible if higher

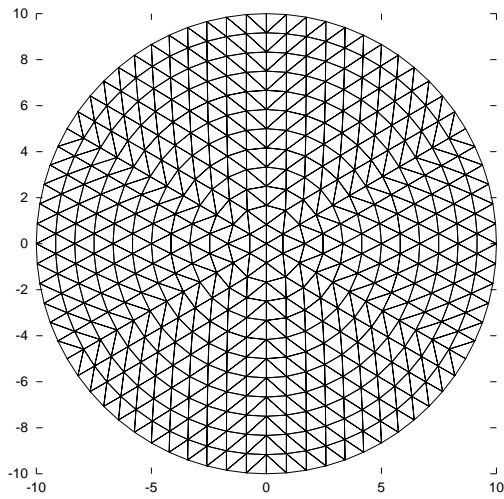


Figure 4: Spatial mesh assumed in calculation.

modes are not damped. Although smoothing by physical or numerical damping enhances the quality of the solution, we can not accept such a technique without restrictions.

The basics of the space–time finite element method was described in [2, 15, 16, 17]. First the displacement formulation was developed. Then the same idea was extended to derive velocity formulas [18, 19, 20, 21].

## 4.2 Example and results

In the numerical analysis of the rolling contact problem we shall limit the investigation to the range where the contact occurs. Other factors such as friction, plastic deformation, hardening, can simply be added following the classical scheme. As an example we take the wheel with the radius  $R=10$  cm, thickness 1 cm, made of steel ( $E=2.05 \cdot 10^7$  N/m<sup>2</sup>,  $\nu=0.3$ ,  $\rho=7.83$  g/cm<sup>3</sup>). It rolls on the rigid base with an angular speed  $\omega$ . The linear velocities taken into account were of the range 90–180 km/h. The elastic material in plane stress was assumed. The domain was discretized with 864 triangles and 469 nodes (Fig. 4). The uniform mesh density was applied for the reason of wave nature of the process and stress concentration passing throughout the domain. To avoid multiple rotations of matrices effected by the rotation of the structure and in the same time the accumulation of round–off errors the rotation of the rigid base over the fixed wheel was assumed. All the forces arising from the circular motion were introduced. In the first stage the wheel, which turns is settled slowly on the rigid base (in numerical simulation the base which

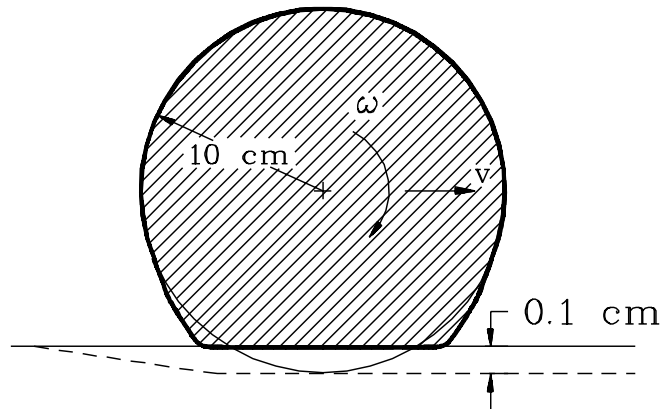


Figure 5: The scheme of the rolling wheel problem.

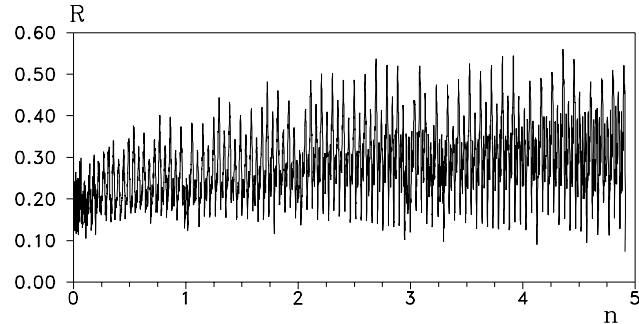
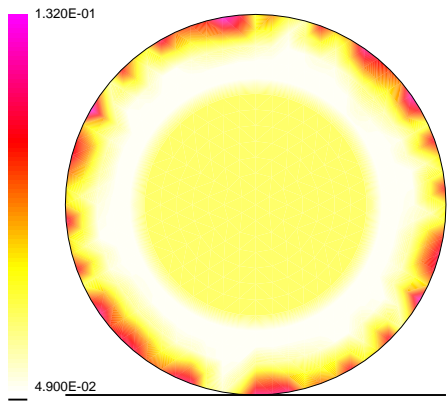


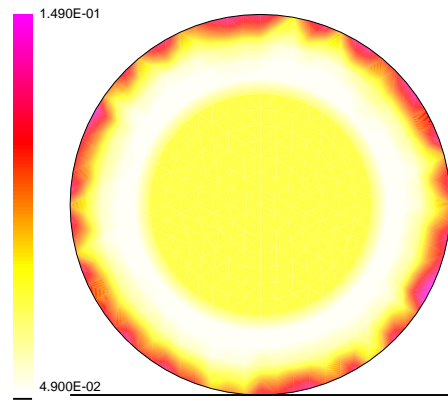
Figure 6: Contact force in successive turns in the case of  $\omega=0.3 \cdot 10^{-3}$  rad/s

turns presses slightly the fixed wheel). The depth of penetration (flattening) reaches finally  $d=0.1$  cm (Fig. 5). In order to avoid the influence of the initial conditions and to reduce the effect of wave reflections and interference the comparatively large numerical damping was assumed. The value of the parameter  $\gamma$  [19] was equal to 0.2 and it corresponded to the logarithmic decrement of damping  $\Lambda = 0.03$ . In practice it allowed to damp vibration according to the first eigenform and the period  $T \approx 80 \mu\text{s}$  in 95% during the first 1/4 turn of the wheel.

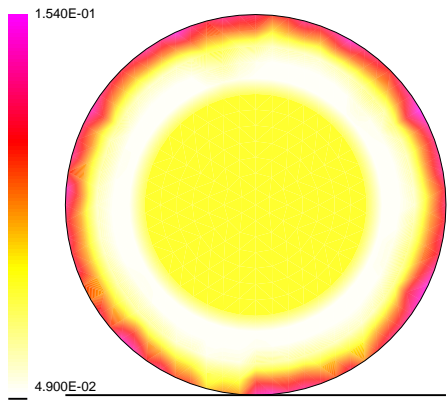
Computation shows that the contact force vary, even when the motion is steady and well damped. First five turns of the wheel with the speed  $\omega=0.3 \cdot 10^{-3}$  rad/s is presented in Fig. 6. The zoom onto the part of the diagram is presented in Fig. 7. The elastic-plastic material with hardening was assumed in computation. The second invariant of stresses  $J_2$  was integrated in successive phases of the full turn. It enables us to show the distribution of stresses in the material (Fig. 8). Final form of the diagram depends on problem parameters.



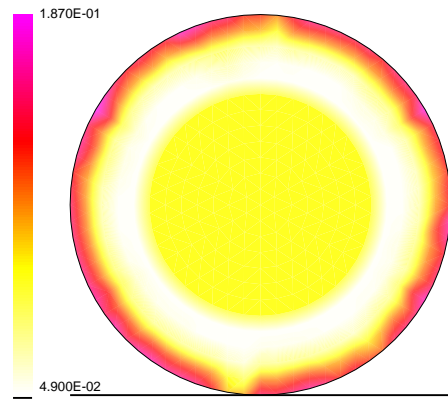
**n=2**



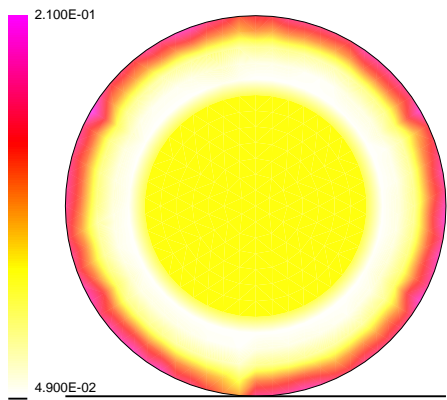
**n=3**



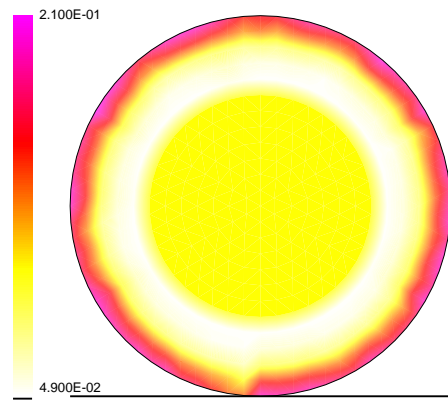
**n=4**



**n=8**



**n=14**



**n=16**

Figure 8: Successive stages of the stress concentrations on the wheel surface

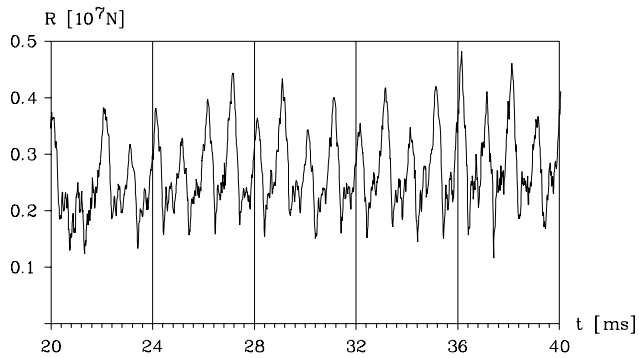


Figure 7: The part of the diagram of the contact force in time.

In the presented example corrugations are successfully flattened. However, in the case of other material coefficients concentrations of stresses under the wheel surface increases.

The analysis exhibits the periodical distribution of the wear on the wheel surface which can occur during exploitation. The number of contact force oscillations decreases along with the increase of the speed. It was observed for example in [22, 23] for a rubber wheel. However, in those publications the authors treat the problem as an eigenvalue problem. They do not solve the initial boundary problem. The estimated diagram of the relation between the number of oscillations in one full turn and the velocity  $\omega$  is shown in Fig. 9. The

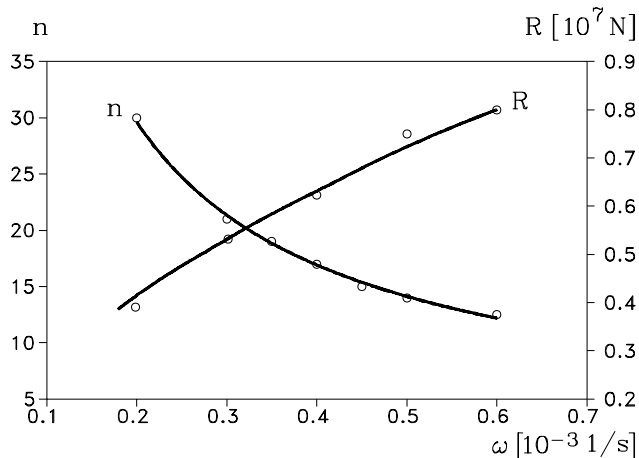


Figure 9: Number of cycles of the reaction and its maximal value in relation of the angular velocity  $\omega$ .

value of the contact force increases with the increase of the velocity  $\omega$ .

The investigation was performed for a full turn of the wheel. If the number of waves due to a turn is

not an integer (*i.e.* the phase shift occurs after each turn), then the diagram is disturbed in the vicinity of the lower point of the wheel, from which the solution starts and on which is finished.

## 5 Conclusions

The efficient method for analysis of dynamic contact problem is presented. The soft way method [19] with modified contact condition described by velocities provides for a convenient treatment of the dynamic contact problem, even in the case of large time steps. The presented method is successfully applied to the problem of corrugations. Even in the simplest case of the material property one can notice the oscillation of the contact force. The resulting stress distribution is stationary if the observation is carried out in the rotating coordinate systems and for the particular value of the angular velocity. If the plastic material was used, the deformation would polygonize the wheel surface permanently. Then successive passages of the wheel over the rail increase the wear by the dynamic feedback [24]. The friction introduced to the contact region can changes quantitative relations. It is shown that neither imperfections of rail junctions nor periodic placement of sleepers generate corrugations. Simple stationary motion is disturbed by the propagation of waves from the contact point. In our case the load is introduced kinematically. In the real problem, despite of different type of loading, the situation can be similar due to considerable inertia of the wheelset.

## References

- [1] R. Bogacz, T. Krzyżyński, and K. Popp. Application of floquet's theorem high-speed train/track dynamics. In *Advanced automotive technologies, ASME Congres*, pages 55–61, 1995.
- [2] C. Bajer, R. Bogacz, and C. Bonthoux. Adaptive space-time elements in the dynamic elastic-viscoplastic problem. *Comput. and Struct.*, 39:415–423, 1991.
- [3] M. Brzozowski, R. Bogacz, and K. Popp. Zur reibungsmodellierung beim rollkontakt (on the modelling of wear in rolling contact). *ZAMM*, pages T678 – T680, 1990.
- [4] R. Bogacz, M. Brzozowski, O. Mahrenholtz, and J. Roñda. Dynamic effects in a rolling contact problem. *ZAMM*, 67(4):T176–T179, 1987.

- [5] R. Bogacz. Residual stresses in high-speed wheel/rail system; Shakedown and corrugations. In A.N.Koanadis, editor, *Proc. of the 1-st European Conference on Steel Structures EUROSTEEL'95*, pages 331–343, Athens, 1995. A,A Balkema.
- [6] Cz. Bajer. Numeryczne modelowanie czasoprzestrzenne dynamicznych zagadnień kontaktowych. Prace IPPT, 5, Warszawa, 1997.
- [7] P. Meinke and T. Szolc. On discrete-continuous modelling in the railway wheelsets for non-linear dynamic analysis in the medium frequency range. In *Proc. 2 Europ. Nonlinear Oscillation Conf., Euro-mech*, pages 135–138, Prague, 1996.
- [8] R. Bogacz and S. Dżuła. Dynamics and stability of a wheelset in rolling contact motion on rails. In *Proc. of ITTG International Symposium on the Technological Innovation in Guided Transports*, pages 871–883, Lille, France, 1993.
- [9] R. Bogacz, T. Krzyzynski, and K. Popp. On the generalization of mathew's problem of the vibration of a beam on elastic foundation. *Z. angew. Math. Mech.*, 69:243–252, 1989.
- [10] S. Dżuła. Free vibration of wheelset wheel. *Arch. Mech. Engng.*, (2/3):97–124, 1989.
- [11] S. Dżuła. Forced vibrations of the rotating railway wheel. *Cracow Univ. of Technology, Selected Problems*, 3:307–323, 1995.
- [12] N.-E. Wiberg, L. Zeng, and X. Li. Error estimation and adaptivity in elastodynamics. *Comput. Meth. Appl. Mech. Engng.*, 101:369–395, 1992.
- [13] L.F. Zeng and N.-E. Wiberg. Spatial mesh adaptation in semidiscrete finite element analysis of linear elastodynamic problems. *Comp. Mech.*, 9(5):315–332, 1992.
- [14] L.F. Zeng, N.-E. Wiberg, and L. Bernspång. An adaptive finite element procedure for 2D dynamic transient analysis using direct integration. *Int. J. Numer. Meth. Engng.*, 34:997–1014, 1992.
- [15] C.I. Bajer. Triangular and tetrahedral space-time finite elements in vibration analysis. *Int. J. Numer. Meth. Engng.*, 23:2031–2048, 1986.
- [16] C.I. Bajer. Notes on the stability of non-rectangular space-time finite elements. *Int. J. Numer. Meth. Engng.*, 24:1721–1739, 1987.
- [17] C.I. Bajer. Adaptive mesh in dynamic problem by the space-time approach. *Comput. and Struct.*, 33(2):319–325, 1989.
- [18] C. Bajer. Space-time finite element formulation for the dynamical evolutionary process. *Appl. Math. and Comp. Sci.*, 3(2):251–268, 1993.
- [19] C. Bajer and C. Bohatier. The soft way method and the velocity formulation. *Comput. and Struct.*, 55(6):1015–1025, 1995.
- [20] C. Bajer and R. Bogacz. New formulation of the space-time finite element method for problems of evolution. *Arch. Mech.*, 46(5):775–788, 1994.
- [21] C. Bohatier and C. Bajer. Kinematic approach for dynamic contact problems — the geometrical soft way method. *Engng. Trans.*, 43(1-2):101–111, 1995.
- [22] J.T. Oden and T.L. Lin. On the general rolling contact problem for finite deformations of viscoelastic cylinder. *Comput. Meth. Appl. Mech. Engng.*, 57:297–367, 1986.
- [23] N. Kikuchi and J.T. Oden. *Contact problems in elasticity: a study of variational inequalities and finite element method*. SIAM, 1988.
- [24] K. Knothe and K. Hempelmann. The formation of corrugation pattern on the rail tread. A linear theory. In *2nd Polish-German Workshop on Dynamical Problems in Mechanical Systems*, pages 77–91, IPPT PAN, Warszawa, 1991.